Published in final edited form as:
Adv Drug Deliv Rev. 2010 August 30; 62(11): 1052–1063. doi:10.1016/j.addr.2010.08.004.

Imaging and drug delivery using theranostic nanoparticles☆

Siti M. Janib[#], **Ara S. Moses**[#], and **J. Andrew MacKay**[*]
Department of Pharmacology and Pharmaceutical Sciences, University of Southern California, Los Angeles, CA 90033-9121, USA

[#] These authors contributed equally to this work.

Abstract

Nanoparticle technologies are significantly impacting the development of both therapeutic and diagnostic agents. At the intersection between treatment and diagnosis, interest has grown in combining both paradigms into clinically effective formulations. This concept, recently coined as theranostics, is highly relevant to agents that target molecular biomarkers of disease and is expected to contribute to personalized medicine. Here we review state-of-the-art nanoparticles from a therapeutic and a diagnostic perspective and discuss challenges in bringing these fields together. Major classes of nanoparticles include, drug conjugates and complexes, dendrimers, vesicles, micelles, core–shell particles, microbubbles, and carbon nanotubes. Most of these formulations have been described as carriers of either drugs or contrast agents. To observe these formulations and their interactions with disease, a variety of contrast agents have been used, including optically active small molecules, metals and metal oxides, ultrasonic contrast agents, and radionuclides. The opportunity to rapidly assess and adjust treatment to the needs of the individual offers potential advantages that will spur the development of theranostic agents.

Keywords

Molecular imaging; Theranostic; Cancer; Chemotherapy; Drug conjugates; Drug complexes; Dendrimers; Vesicles; Micelles; Core–shell; Microbubbles; Carbon nanotubes

1. Introduction

Medical nanotechnology has been developing for decades, and innovative applications are coming to fruition [1]. Nanoparticle formulations, such as Doxil™ and Abraxane™, have demonstrated clinical relevance by increasing drug efficacy and decreasing toxicity, and numerous targeted formulations are under clinical evaluation [2,3]. Some promising applications use nanometer-scale particles for simultaneous drug delivery and molecular imaging. There are unique opportunities to use multifunctional formulations for both diagnostic and therapeutic purposes. This review focuses on the inherent feasibility and practicality of this concept.

Currently, the term ‘theranostics’ encompasses two distinct definitions. We focus on theranostics as defined by the combination of therapeutic and diagnostic agents on a single platform. Specifically, we explore the development of theranostic nanoparticles (TNPs) that

☆This review is part of the *Advanced Drug Delivery Reviews* theme issue on “Development of Theranostic Agents that Co-Deliver Therapeutic and Imaging Agents”.

[*]Corresponding author. Tel.: +1 323 442 4118. jamackay@usc.edu. .

may simultaneously monitor and treat disease. A slightly broader definition has also been proposed, whereby theranostics is defined by use of an appropriate diagnostic methodology to personalize a separate therapeutic intervention [4]. Due to the widespread use of diagnostic tools in clinical decision-making, we have focused on the narrower definition. TNPs offer opportunities to combine passive and active targeting, environmentally-responsive drug release, molecular imaging, and other therapeutic functions into a single platform.

The engineering of multifunctional TNPs will not be straightforward; furthermore, instructive lessons can be gleaned from nearly a half-century of research on nanoparticulate drug carriers. Potential obstacles to successful TNPs include the discovery and targeting of new biomarkers, the innate toxicity of the nanoparticle components, formulation stability, production costs, and control of intellectual property [5,6]. As these new formulations arise, so do large knowledge gaps regarding the safety of nanoparticulates [7]. In addition, optimal therapeutics and diagnostics are two very different entities. Diagnostic (or contrast) agents serve to enhance visibility of specific tissues by increasing the signal to noise ratio relative to surrounding tissues and are generally optimized to provide a quick, high-fidelity snapshot of the living system. Depending upon the wash-in/wash-out kinetics and clearance times of the agent, either a low or high molecular weight (fast or slow clearing) contrast agent can be used [8]. Therapeutic nanoparticle formulations that have been used clinically are commonly long-circulating. This potential discrepancy between fast and slow clearance rates must be reconciled to develop clinically useful TNPs.

The development of effective TNPs will require some give and take between imaging sensitivity, accuracy of targeting, and controlled drug release. Via a host of materials, many pathways are being explored to reach these goals. Currently, the modalities available for imaging of TNPs include optical imaging, magnetic resonance imaging (MRI), nuclear imaging, computed tomography (CT), and ultrasound (US) [9]. Each imaging modality and TNP has relative advantages and disadvantages, which will be discussed.

2. Imaging modality

Molecular imaging allows the characterization of biological processes at the cellular and subcellular levels in intact organisms. By exploiting specific molecular probes or contrast agents, this powerful technique can detect and characterize early stage disease and provide a rapid method for evaluating treatment. Currently used molecular imaging modalities include MRI, CT, US, optical imaging (bioluminescence and fluorescence), single photon emission computed tomography (SPECT) and positron emission tomography (PET) (Fig. 1) [10]. Each imaging modality will be discussed in more detail in the subsequent sections (Table 1).

All of these modalities require a certain quantity of reporter groups to accumulate in a region of interest. Due to the different chemical nature of reporters and intrinsic sensitivity of each technology, the tissue concentration required to achieve signal varies considerably between the modalities. As a platform, nanoparticulates are well-suited for developing targeted contrast agents, because: 1) they have a surface, which can be functionalized with one or more targeting molecules at a wide range of densities; 2) their plasma circulation time can be tuned over several orders of magnitude based on their physico-chemico properties; and 3) contrast agents and drugs can be included at predetermined ratios either in the interior or on the surfaces.

2.1. Optical imaging

Optical imaging is one of the more common modalities used in research. Optical imaging utilizes photons emitted from bioluminescent or fluorescent probes. It has advantages over

other imaging modalities in that the detection of low energy photons is relatively inexpensive; furthermore, the spectrum from visible to near-infrared (NIR) light provides good spatial resolution, without exposure to ionizing radiation. Unfortunately, this modality suffers from poor tissue penetration (0–2 cm) and fluorescent imaging is highly susceptible to noise due to the tissue scattering of photons in the visible light region (395–600 nm) [9]. Optical imaging also suffers from significant background because of tissue autofluorescence and light absorption by proteins (257–280 nm), heme groups (max absorbance at 560 nm), and even water (above 900 nm) [11]. Despite these challenges, the NIR (700–900 nm) window has the advantages of reduced autofluorescence, reduced tissue scattering, and greater depth of penetration, which is most suitable for *in vivo* imaging.

2.2. Magnetic resonance imaging (MRI)

The basis for MRI signal is the precession of water hydrogen nuclei within an applied magnetic field. After application of radiofrequency pulses, the relaxation process through which the nuclei return to the original aligned state can be exploited to produce an image [12]. To enhance the differentiation between tissues, contrast agents are used to shorten the relaxation parameters (T1 and T2) of water. Paramagnetic molecules such as gadolinium (Gd) and manganese (Mn) can be tagged onto small molecules, macromolecules, or nanoparticles. Conversely, magnetic iron-oxide nanoparticles are inherently superparamagnetic and can be tagged at their surfaces with cargo. Compared to radionuclide or optical imaging, MRI has good spatial resolution; however, it suffers from low sensitivity. To offset this, relatively high concentrations of contrast agents are required to produce a detectable signal. The administration of high doses of these contrast agents leads to concerns over accumulation and toxicity, which have become a significant issue for Gd (III) complexes. While Gd (III) provides superior contrast for tumor and vascular imaging, problems with slow excretion and toxicity due to long-term accumulation may hinder its future development in the clinic.

2.3. Radionuclide-based imaging

At the other end of the electromagnetic spectrum, γ-ray emissions are the basis for SPECT and PET. For both modalities, radiopharmaceuticals are administered that can be detected by a camera. Unlike MRI, SPECT and PET images are acquired over a nominally low background signal and require little signal amplification since the gamma rays have energies in the megavolt range. In comparison to PET, SPECT is approximately ten times less sensitive; however, SPECT is advantageous because it enables concurrent imaging of multiple radionuclides. Additionally, SPECT is more widely available than PET, and SPECT radionuclides are simple to prepare and usually have a longer half life than PET radionuclides. SPECT and PET are quantitative techniques, which is an advantage over other modalities such as MRI and optical imaging [13]. Although PET suffers from poor spatial resolution, this can be overcome by hybrid imaging, where PET is used to track molecular events and high resolution CT is used to localize events. While this review specifically focuses on the diagnostic application of radionuclides, it should be noted that certain radionuclides have also been used for radiotherapy [14].

2.4. Computed tomography (CT)

While radionuclide-based imaging is adept at providing information about physiological processes, modalities like CT can provide complementary anatomical information. CT measures the absorption of X-rays as they pass through tissues. The ability of CT to distinguish tissues is based on the fact that different tissues provide distinct degrees of X-ray attenuation, where the attenuation coefficient depends on the atomic number and electron density of the tissues. Differences in absorption between bone, fat, air, and water produce high contrast images of anatomical structures [159].

Currently, CT contrast agents are typically low molecular weight and are characterized by rapid extravasation and clearance. On the other hand, macromolecular and nanoparticulate agents have exhibited superior prolonged presence in the blood pool, which may make them suitable agents for vascular CT. Nanoparticles containing electron dense elements with high atomic number such as iodine, bismuth or gold have been proposed as CT contrast agents [160]. CT contrast requires high concentrations of these elements; therefore, most research is based on solid nanoparticles or liposomes containing iodinated molecules [15]. Gold nanoparticles have gained popularity as CT contrast agents, although it is unclear if gold is an optimal material for physiological use [160,161].

2.5. Ultrasound

US is one of the most common clinical imaging modalities due to its low cost, speed, simplicity, and safety. In this modality, a transducer which emits high frequency sound waves (>20 kHz) is placed against the skin and US images are obtained based on the sound wave reflected back from the internal organs [162]. US contrast agents can improve imaging by introducing a material with different acoustic properties from that of tissues, such as gas [16].

Nanoparticulate-based contrast agents for the imaging modalities discussed are in various stages of development. Typically, the type of nanoparticle used depends on the imaging modality. The next section discusses the types of nanoparticles under development as TNPs.

3. Nanoparticles

By definition, TNPs are multifunctional due to the co-incorporation of both therapeutic and imaging agents. In addition, TNPs may have mechanisms for targeted accumulation, drug activation, or enhancement of contrast. An ideal TNP may have molecular targeting that can be imaged during its circulation in the body. Upon reaching its destination, it may have targeting moieties that associate with cell-surface receptors, internalize into the cytosol, target to the intracellular target if necessary, and release the active therapeutic [17]. Although not all the nanoparticles discussed here will have each of these elements, they illustrate the design-space available to engineer TNPs.

Nanoparticles can be made from a number of materials including proteins, peptides, polymers, lipids, metals and metal oxides, and carbon. While other materials can form nanoparticles, these are the predominant materials under development. The most relevant nanoparticle structures include drug conjugates and complexes, dendrimers, vesicles, micelles, core–shell structures, microbubbles, and carbon nanotubes, which can all be functionalized with a targeting moiety, therapeutic, and contrast agent (Fig. 2). Having been extensively studied as drug carriers, these nanoparticles are being reformulated for co-delivery with imaging agents (Table 2).

3.1. Drug conjugates and complexes

In contrast to self-assembled structures like vesicles and micelles, complexation and covalent conjugation are other direct routes to prepare nanoparticles. Drug complexes rely on reversible interactions between carrier and drug, whereas drug conjugates utilize covalent interactions. Drug conjugates can be prepared using many chemical pathways, which often depends on the chemistry of the drug as well as the carrier. The two major classes of drug conjugates currently under development for theranostic use include protein and peptide-associated and polymer-associated drugs. As with vesicular structures, the effectiveness of a drug conjugate is related to its ability to improve therapeutic index relative to free drug, generally, by reducing toxicity and/or improving efficacy.

Proteins and peptides are versatile materials that can form nanoparticles in several ways, including complexation. The best example of a successful protein nanoparticle already in clinical use is Abraxane™, a formulation of paclitaxel reversibly bound to 130–150 nm albumin nanoparticles via high pressure homogenization [18,19]. Abraxane™ outperformed conventional paclitaxel at an equitoxic dose while decreasing toxicity, due to longer circulation time and decreased offtarget activity [2,18].

Synthetic polypeptides have been used in a similar way. Doxorubicin (Dox) has been chemically conjugated to chimeric polypeptide molecules using thiol chemistry, which drives nanoparticle assembly, increases plasma circulation of drug, and cellular internalization. This increased anti-tumor efficacy and reduced toxicity relative to free drug [20–23]. For drug conjugates and complexes containing Dox, the intrinsic fluorescence of the drug itself may allow optical imaging through thin tissues; however, to make imaging more quantitative it will likely be necessary to modify these conjugates with better contrast agents.

As an alternative to polypeptide polymer, many synthetic polymers have been developed as polymer-drug conjugates. One of the most widely explored polymers is N-(2-hydroxypropyl)methacrylamide (HPMA). HPMA drug conjugates have been studied for over thirty years as HPMA is non-toxic, non-immunogenic, and stable in systemic circulation [24,25]. The goals of polymer-drug conjugation include increasing circulations times, decreasing toxicity, allowing passive tumor targeting, and incorporating various functionalities, such as an active targeting moiety or contrast agent [26–28]. Many different contrast agents have been associated with HPMA copolymer conjugates for *in vitro* and *in vivo* molecular imaging [29]. An HPMA-Dox conjugate labeled with I-131 has even been evaluated in a phase 1 clinical trial [30].

Two schemes for functionalizing HPMA copolymers with diagnostic and therapeutic moieties are via copolymerization and chemical conjugation. While the latter method allows direct conjugation of these contrast agents and therapeutics to the copolymer, it suffers from low conjugation efficiency and difficulty in controlling the degree of conjugation. Even so, two chemotherapeutic agents (Dox and gemcitabine) along with I-131 have been successfully conjugated to a HPMA copolymer using this method [31]. Conversely, copolymerization may be the preferred conjugation method as it offers the flexibility to conjugate both single or multimodal diagnostic agents and chemotherapeutic drugs. An RGD targeted polymer labeled with In-111 and a HPMA construct with Gd was prepared by copolymerization [32,33].

Polymer-drug conjugation is a relatively reliable method to improve pharmacokinetics and increase therapeutic index; non-covalent complexes have a similar effect. Albumin-bound paclitaxel is routinely used in the clinic. The barriers to drug conjugate and complex development into TNPs include the necessity for efficient drug loading and minimization of complexity to control production cost and reliability. Both natural and synthetic polymers are excellent platforms for overcoming these barriers.

3.2. Dendrimers

Polymeric dendrimers are hyperbranched nanostructures that can be controlled in size by controlling the number of polymerization generations. As polymerization progresses, a small, planar molecule transforms into a spherical nanostructure, with cavities where therapeutics and contrast agents can be grafted with great loading efficiency [34]. Dendrimer polymerization and synthesis can be regulated to precisely control the molecular weight and chemical composition of the final product [35]. From the perspective of controlling polymer structure and polydispersity, dendrimers may be ideal platforms for TNPs.

The only dendrimer-based formulation to enter clinical trials thus far is VivaGel™, which uses the dendrimer as a therapeutic agent rather than a carrier — it is currently being evaluated for safety and efficacy as a microbicide [36]. In a recent preclinical study, a fifth generation polyamido-amine (PAMAM) dendrimer conjugated to fluorescein isothiocyanate for imaging and recombinant Fibroblast Growth Factor-1 for tumor targeting was developed to be used to track targeting and cellular internalization [37]. The same group demonstrated a novel release mechanism from a Dox-loaded, folate targeted dendrimer, whereby Dox is conjugated via a photo-sensitive linker, allowing light-controlled drug release [38]. Another group has demonstrated the *in vivo* and *in vitro* efficacy of biodegradable dendrimers, with Dox conjugated via pH-sensitive hydrazone linkers, which showed good biocompatibility, biodistribution, and pharmacokinetics [39–41].

Additions of Gd or iron-oxide are necessary to create a dendrimer-based MRI contrast agent. Wiener and coworkers were the first to demonstrate the viability of dendrimers as MRI contrast agents [42]. The presence of multiple functionalization sites on dendrimers allows attachment of targeting ligands like monoclonal antibodies, peptides and folate [43]. Konda and coworkers, synthesized a fourth generation PAMAM dendrimer with Gd-DTPA chelates. These dendrimers were modified with folic acid to target up-regulated receptors in ovarian cancer [44]. Targeted dendrimers produced site-specific enhanced image contrast and drug localization, in another formulation [45]. To overcome toxicity with macromolecular Gd (III) complexes, Xu and coworkers synthesized a dendrimer with a biodegradable spacer that rapidly eliminates the contrast agent [46]. High relaxivity, efficient loading, and enhancement of tumor and blood pool imaging were observed. Despite encouraging results, the authors concluded that the conjugate is not suitable for further development due to the inherent toxicity of PAMAM dendrimers. Instead, they recommend developing non-toxic, biodegradable dendrimers as a safer alternative which are under development by Szoka and coworkers [35].

The starburst structure of dendrimers allows multivalent attachment of chelators and targeting moieties. Almutairi and coworkers demonstrated highly selective imaging with Br-76 labeled dendritic nanoprobes in an angiogenic mouse model [47]. Attempts have also been made by Kobayashi and coworkers to target delivery of In-111 generation-4 PAMAM dendrimer in a mouse tumor model [48]. Biodistribution indicated rapid blood clearance and preferential accumulation at the tumor site. A similar study by the same group using a second generation PAMAM dendrimer with Y-88 yielded similar results [49]. Yardanov and coworkers characterized an iodinated dendritic nanoparticle, G4-$(DMAA\text{-}IPA)_{37}$ as a CT imaging agent [50]. The construct consists of DMAA-IPA covalently conjugated to a fourth generation PAMAM dendrimer. Due to the multiplicity of DMAA-IPA conjugation, high capacity loading of iodine was achieved, which enhanced contrast for CT.

Dendrimers have been in development for years and have proven to be successful drug and imaging agent carriers in a number of preclinical studies, including, tumor regression, gene delivery, and molecular imaging [6,34,51]. Barriers to address prior to theranostic use of dendrimers include toxicity of the nanoparticle, its polymeric component, as well as the off-target effects of the contrast and therapeutic agent.

3.3. Vesicles

Vesicular structures have been extensively studied as clinical therapeutics and experimentally as diagnostic nanoparticles. The two major classes of vesicles, liposomes and polymer vesicles, have the capacity for covalent and non-covalent encapsulation of both hydrophobic and hydrophilic cargo. Thus, vesicles are well suited to co-deliver therapeutic and diagnostic agents, which can differ in their physicochemico properties. Liposome formulations for therapeutic and diagnostic delivery have been in development for almost

half a century, and have produced clinically successful applications [52]. Polymeric vesicle structures, or polymersomes, have been described more recently, which have unique potential as drug and contrast agent carriers [53].

The best example of a clinical vesicle formulation is Doxil™, also known as liposomal Dox. Encapsulation of Dox in liposomes shielded by polyethylene glycol (PEG) prolongs systemic drug circulation, amplifies safety, and improves the therapeutic index relative to free Dox [6,19]. Moreover, liposomes that co-encapsulate multiple agents are undergoing clinical evaluation. CPX-351, a liposomal formulation with a synergistic molar ratio of 5:1 of cytarabine and daunorubicin, respectively, is currently in Phase II clinical trials for the treatment of acute myeloid leukemia [54]. These liposomes are prepared with cytarabine in the lipid mixture and loaded with daunorubicin after formation, such that the desired loading efficiencies and molar ratios are achieved [55]. Like Doxil™, CPX-351 has prolonged pharmacokinetics, leukemia-selective uptake and cytotoxicity, and improved *in vivo* efficacy, possibly explained by greater drug exposure in the bone marrow and plasma [56,57]. Although CPX-351 is a purely therapeutic formulation, it has been fluorescently labeled and even imaged using the intrinsic fluorescence of the anthracycline, daunorubicin — allowing the possibility of *in vivo* imaging [54,56].

There are multiple examples of liposomal formulations that incorporate targeting, therapeutic, and imaging functionalities [58–62]. As diagnostic agents, liposomes have been labeled with quantum dots (QD) Mn and Gd (both aqueous [63] and chelated [64]), radionuclides such as Ga-67, In-111 and Tc-99 m (anchored to either the lipid bilayer or within the aqueous core), iodine-based agents [15], or even gas (echogenic liposomes [65,66]). As a platform, liposomes can incorporate multiple functionalities without significantly compromising their stability in the body, which makes them suitable nanoparticles for theranostics.

While liposomes are composed from phospholipids chemically similar to those in eukaryotes, some of their most significant enhancements result from polymeric modification. In fact, vesicles can arise from the self-assembly of bilayers composed exclusively from non-lipid polymers. Polymer vesicles or polymersomes have been formed using diblock or triblock copolymers of various polymeric materials including polylactic acid (PLA), polyglycolic acid (PGA), polylactic-co-glycolic acid (PLGA), polycaprolactone (PCL), chitosan, and PEG [67–70]. The principle of these block copolymers is that the hydrophobic block self-associates to form a core membrane, which is stabilized in aqueous media by the hydrophilic polymeric block. As such, polymersomes can encapsulate both hydrophobic and hydrophilic molecules with acceptable encapsulation efficiencies [71–75]. Chemotherapeutic polymersomes carrying Dox and docetaxel have demonstrated improved *in vitro* and *in vivo* efficiency, mediated by controlled release, cellular internalization, and prolonged pharmacokinetics [72,76]. A study demonstrated the specificity of an actively targeted polymeric vesicle via encapsulation and targeted release of a hydrophobic dye [77]. In addition, gene delivery has been demonstrated *in vitro* and *in vivo*, while simultaneously allowing molecular imaging of the polymersome [74,78,79]. Gd-DTPA and iron-oxide loaded PLGA nanoparticles have been used with US and MRI [80,81]. Recently, a construct with similar efficacy and rapid clearance was reported to limit toxicity [82]. Here, superparamagnetic iron-oxide (SPIO) was formulated in nanoparticles consisting of polylactic acid and D-α-tocopherol PEG 1000 succinate. Sequestering the SPIO within this nanoparticle helps to overcome undesirable liver accumulation, which potentially may reduce hepatotoxicity.

Both liposomes and polymersomes are versatile and tunable vehicles for drug delivery and imaging. Many strategies used to form and load liposomes can also be applied to

polymersomes. Furthermore, polymersomes offer enhanced control over the membrane thickness and stability, which may offer pharmaceutical advantages. When incorporating new materials and chemistries on these complex particles, it is important to consider their limitations, such as their inherent production complexity and the vehicle toxicity. Vesicular structures can efficiently load drugs and imaging agents, via either covalent or non-covalent forces, incorporate targeting strategies, prolong systemic circulation, and increase tumor accumulation.

3.4. Micelles

Micellar nanoparticles are attractive structures for carriers of drug and contrast agents because they can form relatively uniform size structures, be prepared from a variety of amphiphilic materials, increase solubility of hydrophobic molecules, and incorporate multiple functionalities into a single structure. Lacking an aqueous core, the drug and contrast agent must be bound to the polymer prior to formation, conjugated to an anchor molecule, or entrapped and associated within the dense, hydrophobic core of the micelle [83]. Micellar structures, including polymeric micelles, have been extensively studied as drug carriers [84].

Like polymersomes or polymer-drug conjugates — similar polymeric materials can be used to form polymeric micelles. In general, a hydrophobic block of the copolymer forms the micellar core, while a hydrophilic portion forms the corona. This corona (commonly consisting of PEG, HPMA, or equivalent hydrophilic polymer) confers these micelles with biocompatibility, stealth-like properties, and a platform for functionalization [85–87]. Genexol-PM™ is a formulation of paclitaxel encapsulated in a polymeric micelle formed by the solid dispersion technique from the biodegradable block copolymer, monomethoxy poly(ethylene glycol)-*block*-poly($_{D,L}$-lactide) [88]. Several clinical trials have already been performed evaluating and validating the safety and efficacy of Genexol-PM™ in metastatic breast cancer, solid tumors, and non-small-cell lung cancer [89–91].

Similarly, contrast-loaded micelles can be used for visualizing numerous organs, tissues and disease sites. Membranotropic chelating agents such as DTPA stearylamine (DTPA-SA) [92] or DTPA-phosphatidylethanolamine (DTPA-PE) [93] have been developed whereby the lipid part of the molecule can be anchored in the micelle's hydrophobic core while a more hydrophilic chelate is localized on the hydrophilic corona. Similarly, polychelating amphiphilic polymers (PAP) that possess multiple side groups for chelation can be anchored to the micellar surface. Different combinations of chelators and hydrophobic anchors have been tested in the preparation of In-111, Tc-99 m and Gd liposomes [94–96]. Chelates with high stability under physiological conditions are preferred so as to avoid toxicity [97–99]. Due to multiplicity of attachment, PAPs can improve image quality at a low micellar dose. Trubetskoy and coworkers incorporated amphiphilic chelating probes (In-111-DTPA-PE and In-111-DTPA-SA) into PEG-PE micelles of 20 nm diameter and used these micelles for γ-scintigraphy of the lymphatic system after subcutaneous administration in rabbits [100]. Moreover, PEG-PE-DTPA micelles labeled with In-111 and an antibody have been used to image a murine model of lung carcinoma [101]. Additionally Trubetskoy and coworkers have also developed iodine-containing micelles for use with CT. Methoxy-polyethylene glycol and tri-iodobenzoic polylysine micelles improved X-ray signal when in rats and rabbits [102].

Due to ease of formation, stability, ability to encapsulate hydrophobic molecules, and therapeutic success in preclinical and clinical studies, polymeric micelles are widely accepted as viable drug and imaging agent delivery systems [86,103–107]. However, the stability of micelles depends on their critical micelle concentration, which makes them prone to exchange their components with other physiological membranes.

3.5. Core–shell

Core–shell structured nanoparticles include particles made with a wide variety of materials including QDs, metals, metal oxides, and polymers among other materials. Their structure resembles a micelle in that there is a core surrounded by a hydrophilic shell. However, most of the core–shell particles relevant to TNPs are stabilized by covalent or ionic bonds, and not hydrophobic effects. There have been advances in the chemical modification of gold and other materials to increase their physiological stability and control drug association and release [17,108]. Core–shell nanoparticles offer stability, modifiable surface properties, and can even produce contrast depending on their composition, size, and shape [109,110].

Metal nanoparticles are attractive options for drug and contrast agent delivery because they are a stable platform on which multiple functionalities can be grafted, some can be imaged directly, and certain formulations allow magnetic-directed guidance [110,111]. The latter can be used to localize drugs, genes, and contrast agents to a specific location. Various SPIO-based nanoparticles have been synthesized that are useful for magnetic guidance, can be imaged, and have surface chemistry that can be modified in order to achieve acceptable biodistributions, while limiting clearance by the reticuloendothelial system (RES) [111]. Also, the superparamagnetism of the iron-oxide nanoparticle allows direct imaging with MRI. SPIO have been widely used to provide contrast for T2 weighted MRI. SPIO can be used alone or attached to other nanostructures.

In a recent study, to demonstrate the viability of these nanoparticles, paclitaxel and a dye were co-encapsulated in the polymer matrix that surrounds the SPIO core. These particles showed dose-dependent internalization and cytotoxicity via multimodal imaging of the dye and SPIO [112]. There are even FDA-approved SPIO nanoparticles, Feraheme™ (Ferumoxytol) is a SPIO nanoparticle with a carbohydrate coating. Feraheme™ can be used for intravascular imaging as well as treating iron deficiency anemia [113,114]. A similar vascular application was reported by Senpan et al. [115]. SPIO can also be manipulated to label specific cell types, for monitoring their *in vivo* behavior [116].

Fluorescent semiconductor QD are nanocrystals consisting of atoms such as cadmium (Cd), zinc (Zn), selenium (Se), telerium (Te), and sulfur (S). However, the most commonly studied QD formulations in biological applications contain a cadmium selenide core and a zinc sulfide shell, which is surrounded by a hydrophilic polymer that can be used to load therapeutics and conjugate targeting ligands [117–119]. QDs can be tuned to emit at between 450 nm to 850 nm by changing their size or chemical composition. QDs improve signal brightness up to 10–100 times when compared to organic fluorophores. Additionally, they have a wide excitation and narrow emission window, fluoresce with high efficiency, and resist photobleaching. Thus far, QDs have also been applied to cancer research in animals, including sentinel node mapping and *in vivo* molecular imaging of tumors [120–124]. QDs have been developed for single molecule labeling, to observe biomolecular dynamics in live cells [125]. The main drawback of QDs is their toxicity. Oxidative degradation of its heavy metal core will lead to the release of metal ions, which bind to sulfyhydryl groups on intracellular proteins and disrupt the function of subcellular organelles.

AuroLase™ is a gold nanoshell formulation in clinical trials for photothermal tumor ablation [126]. The formulation is composed of a gold nanoshell grown around a colloidal silica particle, with thiolated-PEG assembled on the exterior nanoshell surface [127]. After intravenous administration, these nanoparticles passively accumulate in tumor and can be monitored via MRI. After the particles have localized, the tumor is exposed to NIR light, which causes thermal ablation [127]. The *in vivo* imaging and therapeutic effect of this

nanoparticle system has been evaluated in a canine and murine tumor models, and is entering the clinic [126–128].

New synthetic approaches have yielded highly luminescent gold nanoparticles with emissions ranging from 400 to 1200 nm [129,130]. Nanoparticles with this NIR emission makes them suitable for optical imaging as they are less affected by autofluorescence and provide better contrast of the target tissues. Similar to QDs, the emission spectra of gold nanoparticles are size dependent. In addition to optical contrast, gold nanoparticles have been used as CT contrast agents in small animals with little toxicity [131]. Gold is a better CT contrast agent than iodine because gold has a higher atomic number and electron density, which leads to stronger X-ray attenuation and greater contrast. Furthermore, imaging gold at 80–100 keV reduces interference from bone and tissue, which would reduce the radiation exposure to patients. Experiments performed in mice using gold nanoparticles (1.9 nm, ~50 kDa) exhibited good stability, high X-ray absorption, low toxicity, prolonged plasma half life, and enhanced CT contrast of the vasculature, kidneys, and tumor in a mouse model [131].

These core–shell structured nanoparticles make for a very robust therapeutic and contrast agent delivery vehicle due to the vast array of elements that can be used as the core and shell components. Despite the advantages already mentioned, these core–shell nanoparticles suffer from some inherent shortcomings such as toxicity, rapid clearance, and poor biodistribution and biodegradation. Various strategies are in development to circumvent these problems [80,81].

3.6. Microbubbles

Microbubbles and nanobubbles are spherical cavities filled with gas and are usually <10 μM in size. These microbubbles are of varying chemical composition and can be induced to expand and contract (resonate) in the presence of US delivered at the resonance frequency of the microbubbles. The most common gasses used for this purpose in commercially produced contrast agents include perfluorocarbons (PF), such as octofluoropropane (C_3F_8), decafluorobutane (C_4F_{10}) and sulfur hexafluoride (SF_6). The shell encapsulating the gas can be composed of denatured albumin, phospholipids, or various polymers — this shell can then be functionalized to associate with targeting molecules and therapeutics [132,133]. Microbubbles are used as contrast agents for imaging inflammation, angiogenesis, intravascular thrombus and tumors. More recently, microbubbles and nanobubbles are being investigated as potential drug carriers in addition to their role as contrast agents [134].

A study conducted by Gao and coworkers demonstrated the incorporation of Dox into the walls of a polymeric microbubble. PEG-PLLA or PEG-PCL block copolymers were used to form micelles that encapsulate Dox. Then perfluoropentane (PFP) is added and the solution is sonicated — resulting in a mixture of Dox-loaded micelles and Dox-loaded, PFP-encapsulating nanobubbles [135]. As demonstrated *in vitro* and *in vivo* using a murine tumor xenograft model, this Dox-loaded nanobubble/micelle mixture was shown to passively accumulate in tumor tissue and coalesce to form microbubbles, which cavitate and collapse upon tumor-directed US, resulting in drug release [135,136]. This selective accumulation and drug release provided effective Dox delivery and cellular uptake, while simultaneously allowing for molecular imaging of the nano/microbubbles. Another study demonstrates the application of microbubbles for theranostics by using targeted gold nanoparticles to create plasmonic nanobubbles *in situ* after a short laser pulse, which provides contrast for US imaging (diagnostic). This strategy disrupts cellular membranes due to rapid expansion to microbubble size and subsequent collapse upon more laser exposure (therapeutic) [137].

Microbubbles and nanobubbles have been developed as contrast agents for US imaging for a number of years, but their therapeutic potential has recently begun to mature. The use of these nanoparticles as therapeutic agents is still relatively new and requires further evaluation in more complex systems.

3.7. Carbon nanotubes

Carbon nanotubes (CNTs) are cylindrical tubes composed solely of carbon and can either be formed single-walled or multi-walled, for more stability [138]. These CNTs are being investigated as TNPs because of their tunable properties and ability to incorporate multiple functionalities.

Amine-functionalized single-walled CNTs were conjugated via amide linkages to a cisplatin-folic acid derivative as targeted therapeutics, which outperformed a conventional cisplatin formulation [139]. Another study used carboxylated single-walled CNTs to conjugate cisplatin and epidermal growth factor to target cells overexpressing the epidermal growth factor receptor. The targeted CNT-cisplatin conjugate improved the selective killing of the targeted tumor cells [140]. Many studies have confirmed CNTs to be effective carriers of therapeutics and imaging agent *in vitro*, however, *in vivo* studies have lead to concerns regarding the associated toxicities [141–143].

As with QDs and gold nanoparticles, a broad excitation profile and high absorption coefficient can be obtained by tuning CNT over a wide range of wavelengths. Relatively few studies have been conducted utilizing CNTs in optical imaging. However, NIR and Raman signals from CNTs have been detected from within subcutaneous tumors in mice [144]. CNTs provide poor MRI contrast, but they can be functionalized to be made detectable. Richard and coworkers reported functionalization of CNT with amphiphilic Gd (III) chelates and studied their effect on water proton relaxation *in vitro* and *in vivo* [145]. Functionalization of a single-walled CNT surface allows conjugation of In-111 labeled DOTA chelate an anti-CD20 monoclonal antibody for targeted imaging of lymphoid malignancies [146]. A similar study conducted by Liu and coworkers demonstrated that radiolabeled single-walled CNTs can be detected by PET scanning [147]. They also showed that single-walled CNTs conjugated with RGD peptide were able to target and image $\alpha_v\beta_3$ integrin expression in tumors.

CNTs have demonstrated preclinical efficacy for therapeutic and contrast agent delivery — making them interesting nanoparticle formulations for theranostic use. However, the primary barriers that must be overcome include route of biodegradation and reduction of off-target toxicity.

4. Discussion

Most of the contrast agents currently in use consist of low molecular weight compounds that are non-specific, thus making the quantification of diseases at the early stages difficult. The development of nanoparticulate-based contrast agents offers a platform for engineering specificity and sensitivity required for *in vivo* molecular imaging, some examples of these are depicted in Fig. 3. Furthermore, they offer a large surface area, improved circulation time and stability, control over toxicity and targeting [11]. As discussed in the previous sections, these properties are desirable to enhance imaging with high tissue specificity and minimal administration of the contrast agent.

In cancer therapy, one of the principal motivations for developing TNPs is to develop diagnostic and therapeutic agents that are safer and more efficacious. Concurrent *in vivo* imaging allows the detection of tumors at a much earlier stage, which may improve

treatment success and provide treatment efficacy information. The development of TNPs is still in progress, and many barriers must be overcome before they can be translated into the clinic. Certain critical issues need to be addressed such as the safety profile of the TNPs (toxicity and offtarget accumulation), pharmacokinetics and biodistribution (clearance rate, half lives), targeting efficiency (specificity and sensitivity), and biocompatibility (immunogenic response and elimination route). Tackling these issues will bring us closer to developing TNPs that are suitable for clinical use.

Additionally, the therapeutic and diagnostic properties of these agents need to be reconciled. Perhaps the most apparent disparity is the dosage requirements for these two entities. An extreme example given by McCarthy was in the case of TNPs that can potentially be loaded with the radionuclide F-18 and Dox [148]. An imaging dose of 0.5–1.0 μg/kg body weight is usually required to obtain an acceptable signal whereas in the case of Dox a dose of 2 mg/kg is needed for a therapeutic effect. If these agents were to be co-encapsulated, it is conceivable that the patient may not get the required therapeutic dose of Dox at the maximum allowable dose of F-18. Here, the selection of nanoparticle platform may help to overcome these differences. A nanoparticle that has intrinsic imaging and therapeutic properties may be advantageous. For gold (optical imaging) and SPIO (MRI) nanoparticles, the composition itself produces imaging contrast. Moreover, these nanoparticles have therapeutic, thermoablative properties [149,150]. Alternatively TNPs provide a platform for grafting ligands that can increase targeting specificity. A multitude of targeting ligands has been discovered via high throughput screening and phage display. It is expected that these new ligands will improve the affinity and specificity of molecular targeting, hence, allowing better control over local dosing of the TNPs.

Another issue that needs to be resolved is the nature of the contrast agents themselves. On one hand, the requirement for CT usually necessitates the use of a long-circulating contrast agent in order to enhance blood pool imaging. Therefore, using a nanoparticulate-based system could improve upon current contrast. However, the converse is true for MRI contrast agents. Due to the slow excretion rate of macromolecular Gd (III) complexes and the possible toxic accumulation of Gd, it is desirable to have a contrast agent that will be rapidly cleared from the body. In such a case, the type of nanocarriers may be irrelevant if they all contain macromolecular Gd (III) complexes. Accordingly, the safety profile of the respective contrast agents should be carefully considered.

Even though this review has not touched upon it specifically, multimodal nanoparticles that can carry multiple imaging probes suitable for detection by multiple imaging modalities are also being developed. By exploiting the synergistic advantages from different imaging modalities, improved visualization of the biological processes as well as increased reliability of data are possible. Some examples of multimodality imaging being developed include combining fluorescent, MRI, and PET probes. While the rationale for this approach is simple, optimization of two imaging probes without compromising the information from each modality may be a challenge [151].

5. Conclusion

The traditional concept of separating diagnosis and treatment may be in flux. Nanotechnology is blurring the lines between the two entities. Due to the potential advantages that TNPs offer — non-invasive quantification and individualized pharmacotherapy — they represent an exciting opportunity to better manage patients and disease. It is plausible that in the coming years, TNPs will emerge and enter clinical trials. Nanoparticles that can simultaneously detect, image, and treat disease may one day become

the norm rather than the exception. However, before this becomes a reality, issues of safety and complexity must be addressed.

Acknowledgments

This work was aided by the University of Southern California, School of Pharmacy to SMJ, ASM and JAM, by grant IRG-58-007-48 from the American Cancer Society to JAM, and by the Malaysian Public Services Department to SMJ.

Abbreviations

CNT	carbon nanotubes
CT	computed tomography
Dox	doxorubicin
MRI	magnetic resonance imaging
HPMA	N-(2-hydroxypropyl)methacrylamide
NIR	near-infrared
PF	perfluorocarbons
PAA	polyacrylic acid
PAMAM	polyamido-amine
PCL	polycaprolactone
PAP	polychelating amphiphilic polymers
PEG	polyethylene glycol
PGA	polyglycolic acid
PLA	polylactic acid
PLGA	polylactic-co-glycolic acid
PET	positron emission tomography
QD	quantum dot
RES	reticuloendothelial system
SPECT	single photon emission computed tomography
SPIO	superparamagnetic iron-oxide
TNP	theranostic nanoparticle

References

[1]. Whitesides GM. The ‘right’ size in nanobiotechnology. Nat. Biotechnol. 2003; 21:1161–1165. [PubMed: 14520400]

[2]. Miele E, Spinelli GP, Tomao F, Tomao S. Albumin-bound formulation of paclitaxel (Abraxane ABI-007) in the treatment of breast cancer. Int. J. Nanomedicine. 2009; 4:99–105. [PubMed: 19516888]

[3]. Malam Y, Loizidou M, Seifalian AM. Liposomes and nanoparticles: nanosized vehicles for drug delivery in cancer. Trends Pharmacol. Sci. 2009; 30:592–599. [PubMed: 19837467]

[4]. Pene F, Courtine E, Cariou A, Mira JP. Toward theragnostics. Crit. Care Med. 2009; 37:S50–58. [PubMed: 19104225]

[5]. Medina C, Santos-Martinez MJ, Radomski A, Corrigan OI, Radomski MW. Nanoparticles: pharmacological and toxicological significance. Br. J. Pharmacol. 2007; 150:552–558. [PubMed: 17245366]

[6]. Adiseshaiah PP, Hall JB, McNeil SE. Nanomaterial standards for efficacy and toxicity assessment. Wiley Interdiscip. Rev. Nanomed. Nanobiotechnol. 2010; 2:99–112. [PubMed: 20049834]

[7]. Tinkle SS. Maximizing safe design of engineered nanomaterials: the NIH and NIEHS research perspective. Wiley Interdiscip. Rev. Nanomed. Nanobiotechnol. 2010; 2:88–98. [PubMed: 20049833]

[8]. Nahrendorf M, Waterman P, Thurber G, Groves K, Rajopadhye M, Panizzi P, Marinelli B, Aikawa E, Pittet MJ, Swirski FK, Weissleder R. Hybrid in vivo FMT-CT imaging of protease activity in atherosclerosis with customized nanosensors. Arterioscler. Thromb. Vasc. Biol. 2009; 29:1444–1451. [PubMed: 19608968]

[9]. Debbage P, Jaschke W. Molecular imaging with nanoparticles: giant roles for dwarf actors. Histochem. Cell Biol. 2008; 130:845–875. [PubMed: 18825403]

[10]. Massoud TF, Gambhir SS. Molecular imaging in living subjects: seeing fundamental biological processes in a new light. Genes Dev. 2003; 17:545–580. [PubMed: 12629038]

[11]. Park K, Lee S, Kang E, Kim K, Choi K, Kwon IC. New generation of multifunctional nanoparticles for cancer imaging and therapy. Adv. Funct. Mater. 2009; 19:1553–1566.

[12]. Richard C, de Chermont Qle M, Scherman D. Nanoparticles for imaging and tumor gene delivery. Tumori. 2008; 94:264–270. [PubMed: 18564615]

[13]. Beer AJ, Schwaiger M. Imaging of integrin alphavbeta3 expression. Cancer Metastasis Rev. 2008; 27:631–644. [PubMed: 18523730]

[14]. Zalutsky MR, Reardon DA, Pozzi OR, Vaidyanathan G, Bigner DD. Targeted alpha-particle radiotherapy with 211at-labeled monoclonal antibodies. Nucl. Med. Biol. 2007; 34:779–785. [PubMed: 17921029]

[15]. Mukundan S Jr. Ghaghada KB, Badea CT, Kao CY, Hedlund LW, Provenzale JM, Johnson GA, Chen E, Bellamkonda RV, Annapragada A. A liposomal nanoscale contrast agent for preclinical CT in mice. AJR Am. J. Roentgenol. 2006; 186:300–307. [PubMed: 16423931]

[16]. Blomley MJ, Cooke JC, Unger EC, Monaghan MJ, Cosgrove DO. Microbubble contrast agents: a new era in ultrasound. BMJ. 2001; 322:1222–1225. [PubMed: 11358777]

[17]. Haglund E, Seale-Goldsmith MM, Leary JF. Design of multifunctional nanomedical systems. Ann. Biomed. Eng. 2009; 37:2048–2063. [PubMed: 19169822]

[18]. Hawkins MJ, Soon-Shiong P, Desai N. Protein nanoparticles as drug carriers in clinical medicine. Adv. Drug Deliv. Rev. 2008; 60:876–885. [PubMed: 18423779]

[19]. Gaitanis A, Staal S. Liposomal doxorubicin and nab-paclitaxel: nanoparticle cancer chemotherapy in current clinical use. Methods Mol. Biol. 2010; 624:385–392. [PubMed: 20217610]

[20]. Dreher MR, Raucher D, Balu N, Colvin O. Michael, Ludeman SM, Chilkoti A. Evaluation of an elastin-like polypeptide-doxorubicin conjugate for cancer therapy. J. Control. Release. 2003; 91:31–43. [PubMed: 12932635]

[21]. Furgeson DY, Dreher MR, Chilkoti A. Structural optimization of a “Smart” Doxorubicin-polypeptide conjugate for thermally targeted delivery to solid tumors. J. Control. Release. 2006; 110:362–369. [PubMed: 16303202]

[22]. Bidwell GL III, Davis AN, Fokt I, Priebe W, Raucher D. A thermally targeted elastin-like polypeptide-doxorubicin conjugate overcomes drug resistance. Invest New Drugs. 2007; 25:313–326. [PubMed: 17483874]

[23]. Bidwell GL III, Fokt I, Priebe W, Raucher D. Development of elastin-like polypeptide for thermally targeted delivery of doxorubicin. Biochem. Pharmacol. 2007; 73:620–631. [PubMed: 17161827]

[24]. Lammers T, Ulbrich K. HPMA copolymers: 30 years of advances. Adv. Drug Deliv. Rev. 2010; 62:119–121. [PubMed: 20005273]

[25]. Kopecek J, Kopeckova P. HPMA copolymers: origins, early developments, present, and future. Adv. Drug Deliv. Rev. 2010; 62:122–149. [PubMed: 19919846]

[26]. Lammers T. Improving the efficacy of combined modality anticancer therapy using HPMA copolymer-based nanomedicine formulations. Adv. Drug Deliv. Rev. 2010; 62:203–230. [PubMed: 19951732]

[27]. Pike DB, Ghandehari H. HPMA copolymer-cyclic RGD conjugates for tumor targeting. Adv. Drug Deliv. Rev. 2010; 62:167–183. [PubMed: 19951733]

[28]. Pola R, Studenovsky M, Pechar M, Ulbrich K, Hovorka O, Vetvicka D, Rihova B. HPMA-copolymer conjugates targeted to tumor endothelium using synthetic oligopeptides. J. Drug Target. 2009

[29]. Lu ZR. Molecular imaging of HPMA copolymers: visualizing drug delivery in cell, mouse and man. Adv. Drug Deliv. Rev. 2010; 62:246–257. [PubMed: 20060431]

[30]. Vasey PA, Kaye SB, Morrison R, Twelves C, Wilson P, Duncan R, Thomson AH, Murray LS, Hilditch TE, Murray T, Burtles S, Fraier D, Frigerio E, Cassidy J. Phase I clinical and pharmacokinetic study of PK1 [n-(2-hydroxypropyl) methacrylamide copolymer doxorubicin]: first member of a new class of chemotherapeutic agents–drug-polymer conjugates. Cancer research campaign phase I/II committee. Clin. Cancer Res. 1999; 5:83–94. [PubMed: 9918206]

[31]. Lammers T, Subr V, Ulbrich K, Peschke P, Huber PE, Hennink WE, Storm G. Simultaneous delivery of doxorubicin and gemcitabine to tumors in vivo using prototypic polymeric drug carriers. Biomaterials. 2009; 30:3466–3475. [PubMed: 19304320]

[32]. Borgman MP, Coleman T, Kolhatkar RB, Geyser-Stoops S, Line BR, Ghandehari H. Tumor-targeted HPMA copolymer-(RGDfK)-(CHX-A”-DTPA) conjugates show increased kidney accumulation. J. Control. Release. 2008; 132:193–199. [PubMed: 18687371]

[33]. Wang Y, Ye F, Jeong EK, Sun Y, Parker DL, Lu ZR. Noninvasive visualization of pharmacokinetics, biodistribution and tumor targeting of poly[n-(2-hydroxypropyl)methacrylamide] in mice using contrast enhanced mri. Pharm. Res. 2007; 24:1208–1216. [PubMed: 17387601]

[34]. Surendiran A, Sandhiya S, Pradhan SC, Adithan C. Novel applications of nanotechnology in medicine. Indian J. Med. Res. 2009; 130:689–701. [PubMed: 20090129]

[35]. Lee CC, MacKay JA, Frechet JM, Szoka FC. Designing dendrimers for biological applications. Nat. Biotechnol. 2005; 23:1517–1526. [PubMed: 16333296]

[36]. Rupp R, Rosenthal SL, Stanberry LR. Vivagel (spl7013 gel): a candidate dendrimer—microbicide for the prevention of hiv and hsv infection. Int. J. Nanomedicine. 2007; 2:561–566. [PubMed: 18203424]

[37]. Thomas TP, Shukla R, Kotlyar A, Kukowska-Latallo J, Baker JR Jr. Dendrimer-based tumor cell targeting of fibroblast growth factor-1. Bioorg. Med. Chem. Lett. 2010; 20:700–703. [PubMed: 19962894]

[38]. Choi SK, Thomas T, Li MH, Kotlyar A, Desai A, Baker JR Jr. Light-controlled release of caged doxorubicin from folate receptor-targeting pamam dendrimer nanoconjugate. Chem. Commun. (Camb). 2010; 46:2632–2634. [PubMed: 20449327]

[39]. De Jesus, O.L. Padilla; Ihre, HR.; Gagne, L.; Frechet, JM.; Szoka, FC, Jr.. Polyester dendritic systems for drug delivery applications: in vitro and in vivo evaluation. Bioconjug. Chem. 2002; 13:453–461. [PubMed: 12009933]

[40]. Lee CC, Gillies ER, Fox ME, Guillaudeu SJ, Frechet JM, Dy EE, Szoka FC. A single dose of doxorubicin-functionalized bow-tie dendrimer cures mice bearing c-26 colon carcinomas. Proc. Natl Acad. Sci. USA. 2006; 103:16649–16654. [PubMed: 17075050]

[41]. Guillaudeu SJ, Fox ME, Haidar YM, Dy EE, Szoka FC, Frechet JM. Pegylated dendrimers with core functionality for biological applications. Bioconjug. Chem. 2008; 19:461–469. [PubMed: 18173227]

[42]. Wiener EC, Brechbiel MW, Brothers H, Magin RL, Gansow OA, Tomalia DA, Lauterbur PC. Dendrimer-based metal-chelates — a new class of magnetic-resonance-imaging contrast agents. Magn. Reson. Med. 1994; 31:1–8. [PubMed: 8121264]

[43]. Kularatne SA, Low PS. Targeting of nanoparticles: Folate receptor. Methods Mol Biol. 2010; 624:249–265. [PubMed: 20217601]

[44]. Konda SD, Aref M, Wang S, Brechbiel M, Wiener EC. Specific targeting of folate-dendrimer MRI contrast agents to the high affinity folate receptor expressed in ovarian tumor xenografts. Magn. Reson. Mater. Phys., Biol. Med. 2001; 12:104–113.

[45]. Singh P, Gupta U, Asthana A, Jain NK. Folate and folate-PEG-PAMAM dendrimers: synthesis, characterization, and targeted anticancer drug delivery potential in tumor bearing mice. Bioconjug. Chem. 2008; 19:2239–2252. [PubMed: 18950215]

[46]. Xu RZ, Wang YL, Wang XL, Jeong EK, Parker DL, Lu ZR. In vivo evaluation of a PAMAM-cystamine-(Gd-DO3A) conjugate as a biodegradable macromolecular mri contrast agent. Exp. Biol. Med. 2007; 232:1081–1089.

[47]. Almutairi A, Rossin R, Shokeen M, Hagooly A, Ananth A, Capoccia B, Guillaudeu S, Abendschein D, Anderson CJ, Welch MJ, Frechet JM. Biodegradable dendritic positron-emitting nanoprobes for the noninvasive imaging of angiogenesis. Proc. Natl Acad. Sci. USA. 2009; 106:685–690. [PubMed: 19129498]

[48]. Kobayashi H, Sato N, Saga T, Nakamoto Y, Ishimori T, Toyama S, Togashi K, Konishi J, Brechbiel MW. Monoclonal antibody–dendrimer conjugates enable radiolabeling of antibody with markedly high specific activity with minimal loss of immunoreactivity. Eur. J. Nucl. Med. 2000; 27:1334–1339. [PubMed: 11007515]

[49]. Kobayashi H, Wu C, Kim MK, Paik CH, Carrasquillo JA, Brechbiel MW. Evaluation of the in vivo biodistribution of indium-111 and yttrium-88 labeled dendrimer-1B4M-DTPA and its conjugation with anti-Tac monoclonal antibody. Bioconjug. Chem. 1999; 10:103–111. [PubMed: 9893971]

[50]. Yordanov AT, Lodder AL, Woller EK, Cloninger MJ, Patronas N, Milenic D, Brechbiel MW. Novel iodinated dendritic nanoparticles for computed tomography (CT) imaging. Nano Lett. 2002; 2:595–599.

[51]. Mansour HM, Rhee YS, Wu X. Nanomedicine in pulmonary delivery. Int. J. Nanomedicine. 2009; 4:299–319. [PubMed: 20054434]

[52]. Torchilin VP. Recent advances with liposomes as pharmaceutical carriers. Nat. Rev. Drug Discov. 2005; 4:145–160. [PubMed: 15688077]

[53]. Levine DH, Ghoroghchian PP, Freudenberg J, Zhang G, Therien MJ, Greene MI, Hammer DA, Murali R. Polymersomes: a new multi-functional tool for cancer diagnosis and therapy. Methods. 2008; 46:25–32. [PubMed: 18572025]

[54]. Dicko A, Kwak S, Frazier AA, Mayer LD, Liboiron BD. Biophysical characterization of a liposomal formulation of cytarabine and daunorubicin. Int. J. Pharm. 2010; 391:248–259. [PubMed: 20156541]

[55]. Tardi P, Johnstone S, Harasym N, Xie S, Harasym T, Zisman N, Harvie P, Bermudes D, Mayer L. In vivo maintenance of synergistic cytarabine:Daunorubicin ratios greatly enhances therapeutic efficacy. Leuk. Res. 2009; 33:129–139. [PubMed: 18676016]

[56]. Lim WS, Tardi PG, Santos N. Dos, Xie X, Fan M, Liboiron BD, Huang X, Harasym TO, Bermudes D, Mayer LD. Leukemia-selective uptake and cytotoxicity of cpx-351, a synergistic fixed-ratio cytarabine: Daunorubicin formulation, in bone marrow xenografts. Leuk. Res. 2010; 34:1214–1223. [PubMed: 20138667]

[57]. Bayne WF, Mayer LD, Swenson CE. Pharmacokinetics of CPX-351 (cytarabine/daunorubicin HCl) liposome injection in the mouse. J. Pharm. Sci. 2009; 98:2540–2548. [PubMed: 19009594]

[58]. Erdogan S, Torchilin VP. Gadolinium-loaded polychelating polymer-containing tumor-targeted liposomes. Methods Mol. Biol. 2010; 605:321–334. [PubMed: 20072891]

[59]. Al-Jamal WT, Al-Jamal KT, Tian B, Cakebread A, Halket JM, Kostarelos K. Tumor targeting of functionalized quantum dot-liposome hybrids by intravenous administration. Mol. Pharm. 2009; 6:520–530. [PubMed: 19718803]

[60]. Strijkers GJ, Kluza E, Van Tilborg GA, van der Schaft DW, Griffioen AW, Mulder WJ, Nicolay K. Paramagnetic and fluorescent liposomes for target-specific imaging and therapy of tumor angiogenesis. Angiogenesis. 2010; 13:161–173. [PubMed: 20390447]

[61]. Ponce AM, Vujaskovic Z, Yuan F, Needham D, Dewhirst MW. Hyperthermia mediated liposomal drug delivery. Int. J. Hyperthermia. 2006; 22:205–213. [PubMed: 16754340]

[62]. Chen Q, Tong S, Dewhirst MW, Yuan F. Targeting tumor microvessels using doxorubicin encapsulated in a novel thermosensitive liposome. Mol. Cancer Ther. 2004; 3:1311–1317. [PubMed: 15486198]

[63]. Unger EC, Winokur T, MacDougall P, Rosenblum J, Clair M, Gatenby R, Tilcock C. Hepatic metastases: liposomal Gd-DTPA-enhanced MR imaging. Radiology. 1989; 171:81–85. [PubMed: 2928550]

[64]. Trubetskoy VS, Cannillo JA, Milshtein A, Wolf GL, Torchilin VP. Controlled delivery of Gd-containing liposomes to lymph nodes: surface modification may enhance MRI contrast properties. Magn. Reson. Imaging. 1995; 13:31–37. [PubMed: 7534860]

[65]. Alkan-Onyuksel H, Demos SM, Lanza GM, Vonesh MJ, Klegerman ME, Kane BJ, Kuszak J, McPherson DD. Development of inherently echogenic liposomes as an ultrasonic contrast agent. J. Pharm. Sci. 1996; 85:486–490. [PubMed: 8742939]

[66]. Demos SM, Onyuksel H, Gilbert J, Roth SI, Kane B, Jungblut P, Pinto JV, McPherson DD, Klegerman ME. In vitro targeting of antibody-conjugated echogenic liposomes for site-specific ultrasonic image enhancement. J. Pharm. Sci. 1997; 86:167–171. [PubMed: 9040090]

[67]. Discher BM, Won YY, Ege DS, Lee JC, Bates FS, Discher DE, Hammer DA. Polymersomes: tough vesicles made from diblock copolymers. Science. 1999; 284:1143–1146. [PubMed: 10325219]

[68]. Discher DE, Eisenberg A. Polymer vesicles. Science. 2002; 297:967–973. [PubMed: 12169723]

[69]. Jain JP, Kumar N. Self assembly of amphiphilic (PEG)(3)-PLA copolymer as polymersomes: preparation, characterization, and their evaluation as drug carrier. Biomacromolecules. 2010; 11:1027–1035. [PubMed: 20178378]

[70]. Giacomelli C, Schmidt V, Aissou K, Borsali R. Block copolymer systems: from single chain to self-assembled nanostructures. Langmuir. 2010

[71]. Upadhyay KK, Le Meins JF, Misra A, Voisin P, Bouchaud V, Ibarboure E, Schatz C, Lecommandoux S. Biomimetic doxorubicin loaded polymersomes from hyaluronan-block-poly(gamma-benzyl glutamate) copolymers. Biomacromolecules. 2009; 10:2802–2808. [PubMed: 19655718]

[72]. Upadhyay KK, Bhatt AN, Castro E, Mishra AK, Chuttani K, Dwarakanath BS, Schatz C, Le Meins JF, Misra A, Lecommandoux S. In vitro and in vivo evaluation of docetaxel loaded biodegradable polymersomes. Macromol. Biosci. 2010; 10:503–512. [PubMed: 20232310]

[73]. Meng F, Engbers GH, Feijen J. Biodegradable polymersomes as a basis for artificial cells: encapsulation, release and targeting. J. Control. Release. 2005; 101:187–198. [PubMed: 15588904]

[74]. Christian DA, Cai S, Bowen DM, Kim Y, Pajerowski JD, Discher DE. Polymersome carriers: from self-assembly to siRNA and protein therapeutics. Eur. J. Pharm. Biopharm. 2009; 71:463–474. [PubMed: 18977437]

[75]. Upadhyay KK, Bhatt AN, Castro E, Mishra AK, Chuttani K, Dwarakanath BS, Schatz C, Le Meins JF, Misra A, Lecommandoux S. In vitro and in vivo evaluation of docetaxel loaded biodegradable polymersomes. Macromol. Biosci. 2010; 10:503–512. [PubMed: 20232310]

[76]. Upadhyay KK, Bhatt AN, Mishra AK, Dwarakanath BS, Jain S, Schatz C, Le Meins JF, Farooque A, Chandraiah G, Jain AK, Misra A, Lecommandoux S. The intracellular drug delivery and anti tumor activity of doxorubicin loaded poly (gamma-benzyl l-glutamate)-B-hyaluronan polymersomes. Biomaterials. 2010; 31:2882–2892. [PubMed: 20053435]

[77]. Mei H, Shi W, Pang Z, Wang H, Lu W, Jiang X, Deng J, Guo T, Hu Y. EGFP-EGF1 protein-conjugated PEG-PLA nanoparticles for tissue factor targeted drug delivery. Biomaterials. 2010; 31:5619–5626. [PubMed: 20413154]

[78]. Kim Y, Tewari M, Pajeroski DJ, Sen S, Jason W, Sirsi S, Lutz G, Discher DE. Efficient nuclear delivery and nuclear body localization of antisense oligonucleotides using degradable polymersomes. Conf. Proc. IEEE Eng. Med. Biol. Soc. 2006; 1:4350–4353. [PubMed: 17947079]

[79]. Kim Y, Tewari M, Pajerowski JD, Cai S, Sen S, Williams JH, Sirsi SR, Lutz GJ, Discher DE. Polymersome delivery of siRNA and antisense oligonucleotides. J. Control. Release. 2009; 134:132–140. [PubMed: 19084037]

[80]. Ao M, Wang Z, Ran H, Guo D, Yu J, Li A, Chen W, Wu W, Zheng Y. Gd-DTPA-loaded PLGA microbubbles as both ultrasound contrast agent and MRI contrast agent—a feasibility research. J Biomed Mater Res B Appl Biomater. 2010; 93:551–556. [PubMed: 20225249]

[81]. Lee SJ, Jeong JR, Shin SC, Kim JC, Chang YH, Chang YM, Kim JD. Nanoparticles of magnetic ferric oxides encapsulated with poly(D, L latide-co-glycolide) and their applications to magnetic resonance imaging contrast agent. J. Magn. Magn. Mater. 2004; 272–76:2432–2433.

[82]. Prashant C, Dipak M, Yang CT, Chuang KH, Jun D, Feng SS. Superparamagnetic iron oxide–loaded poly(lactic acid)-D-alpha-tocopherol polyethylene glycol 1000 succinate copolymer nanoparticles as mri contrast agent. Biomaterials. 2010; 31:5588–5597. [PubMed: 20434210]

[83]. Liu J, Lee H, Allen C. Formulation of drugs in block copolymer micelles: drug loading and release. Curr. Pharm. Des. 2006; 12:4685–4701. [PubMed: 17168772]

[84]. Torchilin VP. Micellar nanocarriers: pharmaceutical perspectives. Pharm. Res. 2007; 24:1–16. [PubMed: 17109211]

[85]. Torchilin VP. Targeted polymeric micelles for delivery of poorly soluble drugs. Cell. Mol. Life Sci. 2004; 61:2549–2559. [PubMed: 15526161]

[86]. Talelli M, Rijcken CJ, van Nostrum CF, Storm G, Hennink WE. Micelles based on HPMA copolymers. Adv. Drug Deliv. Rev. 2010; 62:231–239. [PubMed: 20004693]

[87]. Nasongkla N, Bey E, Ren J, Ai H, Khemtong C, Guthi JS, Chin SF, Sherry AD, Boothman DA, Gao J. Multifunctional polymeric micelles as cancer-targeted. MRI-ultrasensitive drug delivery systems, Nano Lett. 2006; 6:2427–2430.

[88]. Kim SC, Kim DW, Shim YH, Bang JS, Oh HS, Kim S. Wan, Seo MH. In vivo evaluation of polymeric micellar paclitaxel formulation: toxicity and efficacy. J. Control. Release. 2001; 72:191–202. [PubMed: 11389998]

[89]. Lee KS, Chung HC, Im SA, Park YH, Kim CS, Kim SB, Rha SY, Lee MY, Ro J. Multicenter phase II trial of Genexol-PM, a Cremophor-free, polymeric micelle formulation of paclitaxel, in patients with metastatic breast cancer. Breast Cancer Res. Treat. 2008; 108:241–250. [PubMed: 17476588]

[90]. Kim DW, Kim SY, Kim HK, Kim SW, Shin SW, Kim JS, Park K, Lee MY, Heo DS. Multicenter phase II trial of Genexol-PM, a novel Cremophor-free, polymeric micelle formulation of paclitaxel, with cisplatin in patients with advanced non-small-cell lung cancer. Ann. Oncol. 2007; 18:2009–2014. [PubMed: 17785767]

[91]. Lim WT, Tan EH, Toh CK, Hee SW, Leong SS, Ang PC, Wong NS, Chowbay B. Phase I pharmacokinetic study of a weekly liposomal paclitaxel formulation (Genexol-PM) in patients with solid tumors. Ann. Oncol. 2010; 21:382–388. [PubMed: 19633055]

[92]. Kabalka GW, Davis MA, Holmberg E, Maruyama K, Huang L. Gadolinium-labeled liposomes containing amphiphilic Gd-DTPA derivatives of varying chain-length — targeted MRI contrast enhancement agents for the liver. Magn. Reson. Imaging. 1991; 9:373–377. [PubMed: 1881256]

[93]. Schwendener RA, Wuthrich R, Duewell S, Wehrli E, von Schulthess GK. A pharmacokinetic and MRI study of unilamellar gadolinium-, manganese-, and iron-DTPA-stearate liposomes as organ-specific contrast agents. Invest Radiol. 1990; 25:922–932. [PubMed: 2394576]

[94]. Kabalka GW, Davis MA, Holmberg E, Maruyama K, Huang L. Gadolinium-labeled liposomes containing amphiphilic Gd-DTPA derivatives of varying chain length: targeted MRI contrast enhancement agents for the liver. Magn. Reson. Imaging. 1991; 9:373–377. [PubMed: 1881256]

[95]. Schwendener RA, Wüthrich R, Duewell S, Westera G, von Schulthess GK. Small unilamellar liposomes as magnetic resonance contrast agents loaded with paramagnetic Mn-, Gd-, and Fe-DTPA – stearate complexes. Int. J. Pharm. 1989; 49:249–259.

[96]. Jaggi M, Khar RK, Chauhan UPS, Gangal SV. Liposomes as carriers of 99mTc glucoheptonate for liver imaging. Int. J. Pharm. 1991; 69:77–79.

[97]. Di Bartolo N, Sargeson AM, Smith SV. New 64Cu PET imaging agents for personalised medicine and drug development using the hexa-aza cage. SarAr, Org. Biomol. Chem. 2006; 4:3350–3357.

[98]. Voss SD, Smith SV, DiBartolo N, McIntosh LJ, Cyr EM, Bonab AA, Dearling JL, Carter EA, Fischman AJ, Treves ST, Gillies SD, Sargeson AM, Huston JS, Packard AB. Positron emission

tomography (PET) imaging of neuroblastoma and melanoma with 64Cu-SarAr immunoconjugates. Proc. Natl Acad. Sci. USA. 2007; 104:17489–17493. [PubMed: 17954911]

[99]. Cai H, Li Z, Huang CW, Park R, Shahinian AH, Conti PS. An improved synthesis and biological evaluation of a new cage-like bifunctional chelator, 4-((8-amino-3,6,10,13,16,19-hexaazabicyclo[6.6.6]icosane-1-ylamino)methyl) benzoic acid, for 64Cu radiopharmaceuticals. Nucl Med Biol. 2010; 37:57–65. [PubMed: 20122669]

[100]. Trubetskoy VS, Frank-Kamenetsky MD, Whiteman KR, Wolf GL, Torchilin VP. Stable polymeric micelles: lymphangiographic contrast media for gamma scintigraphy and magnetic resonance imaging. Acad. Radiol. 1996; 3:232–238. [PubMed: 8796670]

[101]. Weissig V, Whiteman KR, Torchilin VP. Accumulation of protein-loaded long-circulating micelles and liposomes in subcutaneous Lewis lung carcinoma in mice. Pharm. Res. 1998; 15:1552–1556. [PubMed: 9794497]

[102]. Trubetskoy VS, Gazelle GS, Wolf GL, Torchilin VP. Block-copolymer of polyethylene glycol and polylysine as a carrier of organic iodine: design of long-circulating particulate contrast medium for X-ray computed tomography. J. Drug Target. 1997; 4:381–388. [PubMed: 9239578]

[103]. Nurunnabi M, Cho KJ, Choi JS, Huh KM, Lee YK. Targeted near-IR QDs-loaded micelles for cancer therapy and imaging. Biomaterials. 2010; 31:5436–5444. [PubMed: 20409581]

[104]. Trivedi R, Kompella UB. Nanomicellar formulations for sustained drug delivery: strategies and underlying principles. Nanomedicine (Lond). 2010; 5:485–505. [PubMed: 20394539]

[105]. Zhang W, Li Y, Liu L, Sun Q, Shuai X, Zhu W, Chen Y. Amphiphilic toothbrushlike copolymers based on poly(ethylene glycol) and poly(epsilon-caprolactone) as drug carriers with enhanced properties. Biomacromolecules. 2010; 11:1331–1338. [PubMed: 20405912]

[106]. Akiba I, Terada N, Hashida S, Sakurai K, Sato T, Shiraishi K, Yokoyama M, Masunaga H, Ogawa H, Ito K, Yagi N. Encapsulation of a hydrophobic drug into a polymer-micelle core explored with synchrotron SAXS. Langmuir. 2010; 26:7544–7551. [PubMed: 20361731]

[107]. Li Y, Xiao K, Luo J, Lee J, Pan S, Lam KS. A novel size-tunable nanocarrier system for targeted anticancer drug delivery. J. Control. Release. 2010; 144:314–323. [PubMed: 20211210]

[108]. Liu S, Han MY. Silica-coated metal nanoparticles. Chem. Asian J. 2010; 5:36–45. [PubMed: 19768718]

[109]. Wei A, Leonov AP, Wei Q. Gold nanorods: multifunctional agents for cancer imaging and therapy. Methods Mol. Biol. 2010; 624:119–130. [PubMed: 20217592]

[110]. Sokolov K, Tam J, Travis K, Larson T, Aaron J, Harrison N, Emelianov S, Johnston K. Cancer imaging and therapy with metal nanoparticles. Conf. Proc. IEEE. Eng. Med. Biol. Soc. 2009; 2009:2005–2007. [PubMed: 19964034]

[111]. Shubayev VI, Pisanic TR II, Jin S. Magnetic nanoparticles for theragnostics. Adv. Drug Deliv. Rev. 2009; 61:467–477. [PubMed: 19389434]

[112]. Santra S, Kaittanis C, Grimm J, Perez JM. Drug/dye-loaded, multifunctional iron oxide nanoparticles for combined targeted cancer therapy and dual optical/magnetic resonance imaging. Small. 2009; 5:1862–1868. [PubMed: 19384879]

[113]. Schwenk MH. Ferumoxytol: a new intravenous iron preparation for the treatment of iron deficiency anemia in patients with chronic kidney disease. Pharmacotherapy. 2010; 30:70–79. [PubMed: 20030475]

[114]. Lu M, Cohen MH, Rieves D, Pazdur R. FDA report: ferumoxytol for intravenous iron therapy in adult patients with chronic kidney disease. Am. J. Hematol. 2010; 85:315–319. [PubMed: 20201089]

[115]. Senpan A, Caruthers SD, Rhee I, Mauro NA, Pan D, Hu G, Scott MJ, Fuhrhop RW, Gaffney PJ, Wickline SA, Lanza GM. Conquering the dark side: colloidal iron oxide nanoparticles. ACS Nano. 2009; 3:3917–3926. [PubMed: 19908850]

[116]. Pittet MJ, Swirski FK, Reynolds F, Josephson L, Weissleder R. Labeling of immune cells for in vivo imaging using magnetofluorescent nanoparticles. Nat. Protoc. 2006; 1:73–79. [PubMed: 17406214]

[117]. Pan J, Liu Y, Feng SS. Multifunctional nanoparticles of biodegradable copolymer blend for cancer diagnosis and treatment. Nanomedicine (Lond). 2010; 5:347–360. [PubMed: 20394529]

[118]. Yildiz I, McCaughan B, Cruickshank SF, Callan JF, Raymo FM. Biocompatible CdSe-ZnS core–shell quantum dots coated with hydrophilic polythiols. Langmuir. 2009; 25:7090–7096. [PubMed: 19239226]

[119]. Yildiz I, Deniz E, McCaughan B, Cruickshank SF, Callan JF, Raymo FM. Hydrophilic CdSe-ZnS core–shell quantum dots with reactive functional groups on their surface. Langmuir. 2010; 26:11503–11511. [PubMed: 20455526]

[120]. Ballou B, Ernst LA, Andreko S, Harper T, Fitzpatrick JA, Waggoner AS, Bruchez MP. Sentinel lymph node imaging using quantum dots in mouse tumor models. Bioconjug. Chem. 2007; 18:389–396. [PubMed: 17263568]

[121]. Kim S, Lim YT, Soltesz EG, De Grand AM, Lee J, Nakayama A, Parker JA, Mihaljevic T, Laurence RG, Dor DM, Cohn LH, Bawendi MG, Frangioni JV. Near-infrared fluorescent type II quantum dots for sentinel lymph node mapping. Nat. Biotechnol. 2004; 22:93–97. [PubMed: 14661026]

[122]. Gao X, Cui Y, Levenson RM, Chung LW, Nie S. In vivo cancer targeting and imaging with semiconductor quantum dots. Nat. Biotechnol. 2004; 22:969–976. [PubMed: 15258594]

[123]. Wu X, Liu H, Liu J, Haley KN, Treadway JA, Larson JP, Ge N, Peale F, Bruchez MP. Immunofluorescent labeling of cancer marker Her2 and other cellular targets with semiconductor quantum dots. Nat. Biotechnol. 2003; 21:41–46. [PubMed: 12459735]

[124]. Bentolila LA, Ebenstein Y, Weiss S. Quantum dots for in vivo small-animal imaging. J. Nucl. Med. 2009; 50:493–496. [PubMed: 19289434]

[125]. Chang YP, Pinaud F, Antelman J, Weiss S. Tracking bio-molecules in live cells using quantum dots. J. Biophotonics. 2008; 1:287–298. [PubMed: 19343652]

[126]. O'Neal DP, Hirsch LR, Halas NJ, Payne JD, West JL. Photo-thermal tumor ablation in mice using near infrared-absorbing nanoparticles. Cancer Lett. 2004; 209:171–176. [PubMed: 15159019]

[127]. Schwartz JA, Shetty AM, Price RE, Stafford RJ, Wang JC, Uthamanthil RK, Pham K, McNichols RJ, Coleman CL, Payne JD. Feasibility study of particle-assisted laser ablation of brain tumors in orthotopic canine model. Cancer Res. 2009; 69:1659–1667. [PubMed: 19208847]

[128]. Goodrich GP, Bao L, Gill-Sharp K, Sang KL, Wang J, Payne JD. Photothermal therapy in a murine colon cancer model using near-infrared absorbing gold nanorods. J. Biomed. Opt. 2010; 15:018001. [PubMed: 20210487]

[129]. Montalti M, Zaccheroni N, Prodi L, O'Reilly N, James SL. Enhanced sensitized NIR luminescence from gold nanoparticles via energy transfer from surface-bound fluorophores. J. Am. Chem. Soc. 2007; 129:2418–2419. [PubMed: 17286405]

[130]. Zheng J, Petty JT, Dickson RM. High quantum yield blue emission from water-soluble Au8 nanodots. J. Am. Chem. Soc. 2003; 125:7780–7781. [PubMed: 12822978]

[131]. Hainfeld JF, Slatkin DN, Focella TM, Smilowitz HM. Gold nanoparticles: a new X-ray contrast agent. Br. J. Radiol. 2006; 79:248–253. [PubMed: 16498039]

[132]. Landini L, Santarelli MF, Positano V. Ultrasound techniques for drug delivery in cardiovascular medicine. Curr. Drug Discov. Technol. 2008; 5:328–332. [PubMed: 19075613]

[133]. Krupka TM, Solorio L, Wilson RE, Wu H, Azar N, Exner AA. Formulation and characterization of echogenic lipid-pluronic nanobubbles. Mol. Pharm. 2010; 7:49–59. [PubMed: 19957968]

[134]. Ferrara KW, Borden MA, Zhang H. Lipid-shelled vehicles: engineering for ultrasound molecular imaging and drug delivery. Acc. Chem. Res. 2009; 42:881–892. [PubMed: 19552457]

[135]. Gao Z, Kennedy AM, Christensen DA, Rapoport NY. Drug-loaded nano/microbubbles for combining ultrasonography and targeted chemotherapy. Ultrasonics. 2008; 48:260–270. [PubMed: 18096196]

[136]. Rapoport N, Gao Z, Kennedy A. Multifunctional nanoparticles for combining ultrasonic tumor imaging and targeted chemotherapy. J. Natl Cancer Inst. 2007; 99:1095–1106. [PubMed: 17623798]

[137]. Lukianova-Hleb EY, Hanna EY, Hafner JH, Lapotko DO. Tunable plasmonic nanobubbles for cell theranostics. Nanotechnology. 2010; 21:85102. [PubMed: 20097970]

[138]. Dennany L, Sherrell P, Chen J, Innis PC, Wallace GG, Minett AI. Epr characterisation of platinum nanoparticle functionalised carbon nanotube hybrid materials. Phys. Chem. Chem. Phys. 2010; 12:4135–4141. [PubMed: 20379504]

[139]. Dhar S, Liu Z, Thomale J, Dai H, Lippard SJ. Targeted single-wall carbon nanotube-mediated Pt(IV) prodrug delivery using folate as a homing device. J. Am. Chem. Soc. 2008; 130:11467–11476. [PubMed: 18661990]

[140]. Bhirde AA, Patel V, Gavard J, Zhang G, Sousa AA, Masedunskas A, Leapman RD, Weigert R, Gutkind JS, Rusling JF. Targeted killing of cancer cells in vivo and in vitro with EGF-directed carbon nanotube-based drug delivery. ACS Nano. 2009; 3:307–316. [PubMed: 19236065]

[141]. Shvedova AA, Kagan VE. The role of nanotoxicology in realizing the 'helping without harm' paradigm of nanomedicine: lessons from studies of pulmonary effects of single-walled carbon nanotubes. J. Intern. Med. 2010; 267:106–118. [PubMed: 20059647]

[142]. Sanchez-Cano C, Hannon MJ. Novel and emerging approaches for the delivery of metallo-drugs. Dalton Trans. 2009:10702–10711. [PubMed: 20023897]

[143]. Aillon KL, Xie Y, El-Gendy N, Berkland CJ, Forrest ML. Effects of nanomaterial physicochemical properties on in vivo toxicity. Adv. Drug Deliv. Rev. 2009; 61:457–466. [PubMed: 19386275]

[144]. Keren S, Zavaleta C, Cheng Z, de la Zerda A, Gheysens O, Gambhir SS. Noninvasive molecular imaging of small living subjects using Raman spectroscopy. Proc. Natl Acad. Sci. USA. 2008; 105:5844–5849. [PubMed: 18378895]

[145]. Richard C, Doan BT, Beloeil JC, Bessodes M, Toth E, Scherman D. Noncovalent functionalization of carbon nanotubes with amphiphilic Gd3+ chelates: toward powerful T1 and T2 MRI contrast agents. Nano Lett. 2008; 8:232–236. [PubMed: 18088153]

[146]. McDevitt MR, Chattopadhyay D, Kappel BJ, Jaggi JS, Schiffman SR, Antczak C, Njardarson JT, Brentjens R, Scheinberg DA. Tumor targeting with antibody-functionalized, radiolabeled carbon nanotubes. J. Nucl. Med. 2007; 48:1180–1189. [PubMed: 17607040]

[147]. Liu Z, Cai W, He L, Nakayama N, Chen K, Sun X, Chen X, Dai H. In vivo biodistribution and highly efficient tumour targeting of carbon nanotubes in mice. Nat. Nanotechnol. 2007; 2:47–52. [PubMed: 18654207]

[148]. McCarthy JR. The future of theranostic nanoagents. Nanomedicine. 2009; 4:693–695. [PubMed: 19839803]

[149]. DeNardo SJ, DeNardo GL, Natarajan A, Miers LA, Foreman AR, Gruettner C, Adamson GN, Ivkov R. Thermal dosimetry predictive of efficacy of In-111-Chl6 nanoparticle AMF-induced thermoablative therapy for human breast cancer in mice. J. Nucl. Med. 2007; 48:437–444. [PubMed: 17332622]

[150]. DeNardo SJ, Richman CM, Albrecht H, Burke PA, Natarajan A, Yuan A, Gregg JP, O'Donnel RT, DeNardo GL. Enhancement of the therapeutic index: from nonmyeloablative and myeloablative toward pretargeted radioimmunotherapy for metastatic prostate cancer. Clin. Cancer Res. 2005; 11:7187 s–7194 s.

[151]. Lucignani G. Nanoparticles for concurrent multimodality imaging and therapy: the dawn of new theragnostic synergies. Eur. J. Nucl. Med. Mol. Imaging. 2009; 36:869–874. [PubMed: 19288097]

[152]. Baiker M, Milles J, Dijkstra J, Henning TD, Weber AW, Que I, Kaijzel EL, Lowik CW, Reiber JH, Lelieveldt BP. Atlas-based whole-body segmentation of mice from low-contrast micro-CT data. Med Image Anal. 2010; 14:723–737. [PubMed: 20576463]

[153]. Radu CG, Shu CJ, Nair–Gill E, Shelly SM, Barrio JR, Satyamurthy N, Phelps ME, Witte ON. Molecular imaging of lymphoid organs and immune activation by positron emission tomography with a new [18F]-labeled 2′-deoxycytidine analog. Nat. Med. 2008; 14:783–788. [PubMed: 18542051]

[154]. Le LP, Rivera AA, Glasgow JN, Ternovoi VV, Wu H, Wang M, Smith BF, Siegal GP, Curiel DT. Infectivity enhancement for adenoviral transduction of canine osteosarcoma cells. Gene Ther. 2006; 13:389–399. [PubMed: 16292351]

[155]. Snyder CS, Kaushal S, Kono Y, Cao H.S. Tran, Hoffman RM, Bouvet M. Complementarity of ultrasound and fluorescence imaging in an orthotopic mouse model of pancreatic cancer. BMC Cancer. 2009; 9:106. [PubMed: 19351417]

[156]. Yang J, Lee CH, Ko HJ, Suh JS, Yoon HG, Lee K, Huh YM, Haam S. Multifunctional magneto-polymeric nanohybrids for targeted detection and synergistic therapeutic effects on breast cancer. Angew. Chem. Int. Ed Engl. 2007; 46:8836–8839. [PubMed: 17943947]

[157]. Medarova Z, Pham W, Farrar C, Petkova V, Moore A. In vivo imaging of siRNA delivery and silencing in tumors. Nat. Med. 2007; 13:372–377. [PubMed: 17322898]

[158]. Cai W, Shin DW, Chen K, Gheysens O, Cao Q, Wang SX, Gambhir SS, Chen X. Peptide-labeled near-infrared quantum dots for imaging tumor vasculature in living subjects. Nano Lett. 2006; 6:669–676. [PubMed: 16608262]

[159]. Weissleder R. Scaling down imaging: Molecular mapping of cancer in mice. Nat. Rev. Cancer. 2002; 2:11–18. [PubMed: 11902581]

[160]. Cormode DP, Skajaa T, Fayad ZA, Mulder WJ. Nanotechnology in medical imaging: Probe design and applications. Arterioscler. Thromb. Vasc. Biol. 2009; 29:992–1000. [PubMed: 19057023]

[161]. Kim D, Park S, Lee JH, Jeong YY, Jon S. Antibiofouling polymer-coated gold nanoparticles as a contrast agent for in vivo x-ray computed tomography imaging. J. Am. Chem. Soc. 2007; 129:7661–7665. [PubMed: 17530850]

[162]. Massoud TF, Gambhir SS. Molecular imaging in living subjects: Seeing fundamental biological processes in a new light. Genes Dev. 2003; 17:545–580. [PubMed: 12629038]

[163]. Mody VV, Nounou MI, Bikram M. Novel nanomedicine-based mri contrast agents for gynecological malignancies. Adv. Drug Reliv. Rev. 2009; 61:795–807.

[164]. Ventura A, Kirsch DG, McLaughlin ME, Tuveson DA, Grimm J, Lintault L, Newman J, Reczek EE, Weissleder R, Jacks T. Restoration of p53 function leads to tumour regression in vivo. Nature. 2007; 445:661–665. [PubMed: 17251932]

[165]. Fu D-X, Tanhehco Y, Chen J, Foss CA, Fox JJ, Chong J-M, Hobbs RF, Fukayama M, Sgouros G, Kowalski J, Pomper MG, Ambinder RF. Bortezomib-induced enzyme-targeted radiation therapy in herpesvirus-associated tumors. Nature Medicine. 2008; 14:1118–1122.

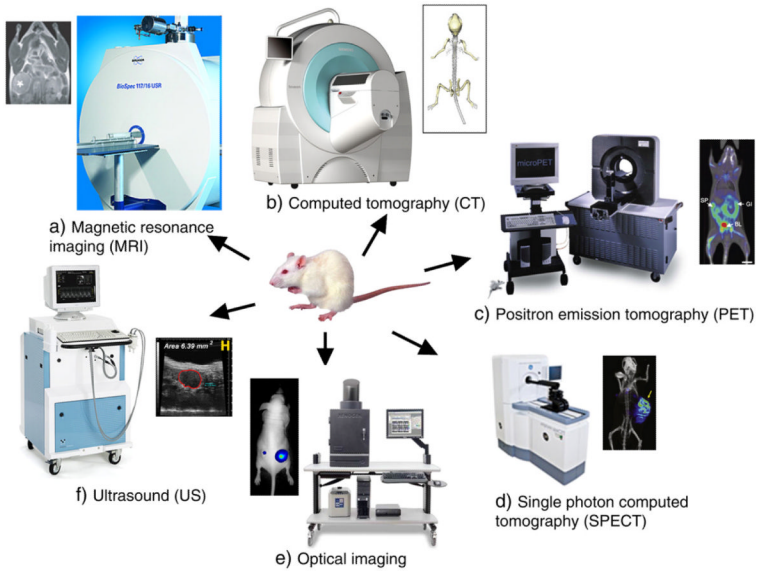

Fig. 1.

Typical molecular imaging instruments and images representative of each modality. a) MRI [reprinted with permission from Macmillan Publishers Ltd: [164], © (2007); Image of instrument courtesy of Bruker Biospin Corporation.], b) computed tomography [reprinted from [152], © (2010) with permission from Elsevier; Image of instrument courtesy of Siemens.], c) positron emission tomography [reprinted by permission from Macmillan Publishers Ltd.: [153], © 2008; Image of instrument courtesy of Siemens.], d) single photon emission computed tomography [Reprinted by permission from Macmillan Publishers Ltd: [165], © (2008); Image of instrument courtesy of GE Healthcare.], e) optical imaging [reprinted by permission from Macmillan Publishers Ltd.: [154], © (2006); Image of instrument courtesy of Caliper Life Sciences.], f) ultrasound [reprinted from 155; Image of instrument courtesy of VisualSonics].

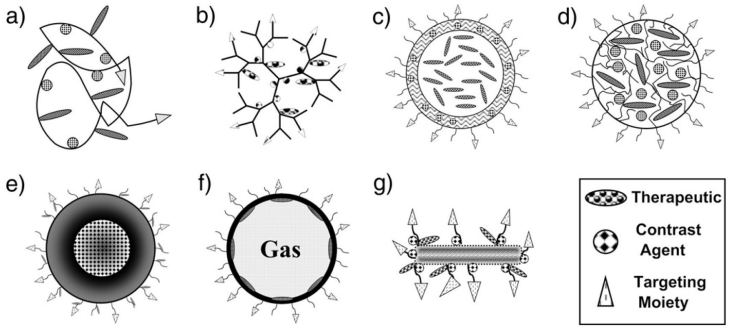

Fig. 2.

Structural representations of nanoparticle classes functionalized for theranostics. Schematics of a functionalized a) drug conjugate; b) dendrimer; c) vesicle; d) micelle; e) core–shell nanoparticle; f) microbubble; and g) carbon nanotube.

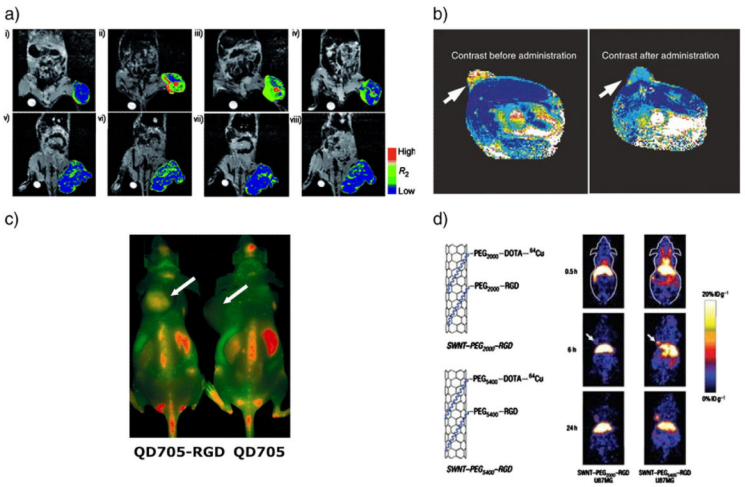

Fig. 3.

Several examples of nanoparticle contrast agents and TNPs. a) MR images and their color maps (tumor region) of cancer-targeting events of antibody (herceptin) directed multifunctional magneto-polymeric nanohybrid (MMPN) (i–iv) and non-targeted MMPNs (v–viii) in NIH3T6.7 cells implanted in mice at various time intervals. Tumor growth inhibition was demonstrated ([156], copyright Wiley–VCH Verlag GmbH & Co. KGaA. Reproduced with permission). b) *In vivo* MRI of mice bearing subcutaneous LS174T human colorectal adenocarcinoma (arrows). A significant drop in T2 relaxivity indicated successful probe delivery (covalently linked siRNA to a magnetic nanoparticle) which induces tumor silencing [reprinted by permission from Macmillan Publishers Ltd.: [157], © (2007). c) *In vivo* NIRF imaging of U87MG tumor-bearing mice injected with 200 pmol of QD705–RGD or QD705. Arrows indicate tumors (reprinted with permission from [158], © 2006 American Chemical Society). d) MicroPET images of two mice at various time points post tailvein injection of 64Cu-labeled single-walled CNT–PEG2000 and single-walled CNT–PEG5400, respectively. The arrows point to the tumors (reprinted by permission from Macmillan Publishers Ltd.: [147], © (2007).

Table 1

Summary of the properties and characteristics of various imaging modalities [162,163].

Imaging modality	Type of probe	Sensitivity (M)	Spatial resolution	Advantages	Disadvantages
Optical imaging	Fluorescent dyes, quantum dots	Bioluminescence — 10^{-15}– to 10^{-17} Fluorescence — 10^{-9} to 10^{-12}	2–5mm	•High sensitivity •Provide functional information •No radiation exposure	•Low resolution •Limited tissue penetration
Computed tomography (CT)	Heavy element e.g. iodine	Not well characterized	50–200 μm	•High spatial resolution. •Ability to differentiate between tissues. •Low radiation exposure	•Require contrast agent for enhanced tissue contrast. •Radiation •Tissue non-specificity •High cost
Magnetic resonance imaging (MRI)	Para- or superparamagnetic metals (e.g. Gd, Mn)	10^{-3} to 10^{-5}	25–100 μm	•High resolution •No ionizing radiation •Able to image physiological and anatomical details	•High cost •Cannot be used in patients with metallic devices e.g. pacemakers
Gamma scintigraphy (PET and SPECT)	Radionuclides (e.g. F-18, In-111, Cu-64)	PET — 10^{-11} to 10^{-12} SPECT — 10^{-10} to 10^{-11}	1–2mm	•Ability to image biochemical processes	•Radiation •Low resolution •Cost
Ultrasound	Gas filled microbubbles	Not well characterized	50–500 μm	•Non-invasive •Ease of procedure •No radiation exposure •Low cost	•Low resolution

Table 2

Examples of theranostic nanoparticles.

Type	Material	Size	Therapeutic	Contrast agent	Targeting	References
Drug conjugate	HPMA	~74 kDa	n.a.	DY-615	Active (RGD)	[27]
Dendrimer	PAMAM-PEG	~100 nm	5-Fluorouracil	5-Fluorouracil	Active (folic acid)	[44]
Vesicle	Poly(g-benzyl L-glutamate)-block-hyaluronan	~260 nm	Docetaxel	Tc-99 m	Passive	[74]
Micelle	PEG-PLA	~45 nm	Dox	SPIO	Active (RGD)	[86]
Core–shell	PAA/SPIO	~90 nm	Paclitaxel	SPIO/DiI	Active (folic acid)	[111]
Microbubble	PEG-PLLA/PFP	~125 nm	Dox	PFP	Passive	[135]
Carbon nanotube	Carbon	~110×10 nm	Cisplatin	QD	Active (epidermal growth factor)	[139]